Peng, X.; Behl, M.; Zhang, P.; Mazurek-Budzynska, M.; Razzaq, M.Y.; Lendlein, A.:

Hexyl-modified morpholine-2,5-dione-based oligodepsipeptides with relatively low glass transition temperature

In: Polymer (2016) Elsevier

DOI: 10.1016/j.polymer.2016.10.033

Hexyl-modified morpholine-2,5-dione-based oligodepsipeptides with relatively low glass transition temperature

Xingzhou Peng[1,2,3,4], Marc Behl[1,3], Pengfei Zhang[1,2,3], Magdalena Mazurek-Budzyńska[1], Muhammad Yasar Razzaq[1], Yakai Feng[3,4], Andreas Lendlein[1,2,3*]

[1] Institute of Biomaterial Science and Berlin-Brandenburg Centre for Regenerative Therapies, Helmholtz-Zentrum Geesthacht, 14513 Teltow, Germany

[2] Institute of Chemistry, University of Potsdam, 14476 Potsdam, Germany

[3]Tianjin University-Helmholtz-Zentrum Geesthacht Joint Laboratory for Biomaterials and Regenerative Medicine, 14513 Teltow, Germany

[4] School of Chemical Engineering and Technology, Tianjin University, Tianjin 300350, China

*Corresponding author. E-mail address: andreas.lendlein@hzg.de

Abstract

Oligodepsipeptides (oDPs), alternating copolymers of an α-amino acid and an α-hydroxy acid, are typically created by ring-opening polymerization (ROP) of morpholine-2,5-dione derivatives (MDs). In general, oDPs exhibit relatively high glass transition temperatures (T_gs) caused by the strong intermolecular H-bonding between amide and ester bonds. So far, it was not reported that variation at α-amino acid moieties in MDs monomers lead to lower T_g. Here we explored whether the thermal properties of the oDPs can be adjusted by introducing a hexyl side chain in the α-hydroxy acid part of the MDs. By synthesizing a MD with an atactic pendant hexyl group at position 3, the influence of a modification at position 6 compared to a modification at position 3 towards ROP was investigated. In both cases the atactic bulky side groups hindered the H-bonding between chain segments resulting in a significant reduction of the T_gs to a temperature around

human body temperature (32 and 36 °C) in contrast to ROP of a MD providing a methyl group at position 3 and a $T_g \approx 65$ °C. Such oDPs could be interesting candidate materials for biomedical applications such as degradable implants.

Introduction

Oligodepsipeptides (oDPs), known as alternating copolymers of an α-amino acid and an α-hydroxy acid, have shown great promise for biomedical applications such as tissue engineering and drug delivery systems [1-5] as the degradation of amide bonds in oDPs is inherently buffered, and by this results in lower immune system response in contrast to the degradation of polyester-based materials causing a substantial decrease of pH.

oDPs can be synthesized using ring-opening polymerization (ROP) of morpholine-2,5-dione (MD) derivatives [6]. A variety of MDs with tunable physical and chemical properties were synthesized by modification of the amino acid moiety, resulting in oDPs with promising applications[7-10]. So far MDs were modified by substitutions at position 3 by varying the α-amino acid moieties; e.g. valine, leucine, isoleucine, and alanine have been used to synthesize isopropyl, isobutyl, *sec*-butyl and methyl substituted MDs [11, 12]. From these, oDPs with controlled molecular weight and designed end functionalities were synthesized by ROP. The mechanism of ROP catalyzed by tin(II) 2-ethylhexanoate ($Sn(Oct)_2$), especially of lactones and cyclic esters, was intensively studied and several theories of ROP mechanisms were discussed [13, 14]. The most commonly accepted mechanism for $Sn(Oct)_2$-catalyzed ROP is the “coordination-insertion” mechanism, in which at first, a tin alkoxide, which is the active species for the ROP, is formed from the $Sn(Oct)_2$ and hydroxyl groups of initiator. Afterwards the tin alkoxide forms a complex with the carbonyl oxygen of the ester group, resulting in a nucleophilic attack of the acyl carbon. The ester bond cleavage goes along with the formation of a new tin-oxygen bonds and results in analogue active

species. Ester bonds in MDs have a higher activity compared to amide bond and act as main functional group during the ROP. In this context, the "coordination-insertion" mechanism is also applicable for the ROP of MDs (Scheme 1). Furthermore, the structure of MD influences the efficiency of ROP during the oDPs synthesis. Recently, the synthesis and polymerization of versatile MDs have been reported, presenting glass transition temperatures (T_gs) of oDPs ranging from 93 °C to 117 °C [11]. Such high T_gs can be attributed to the strong H-bond interactions and high crystallinity in the oligomers.

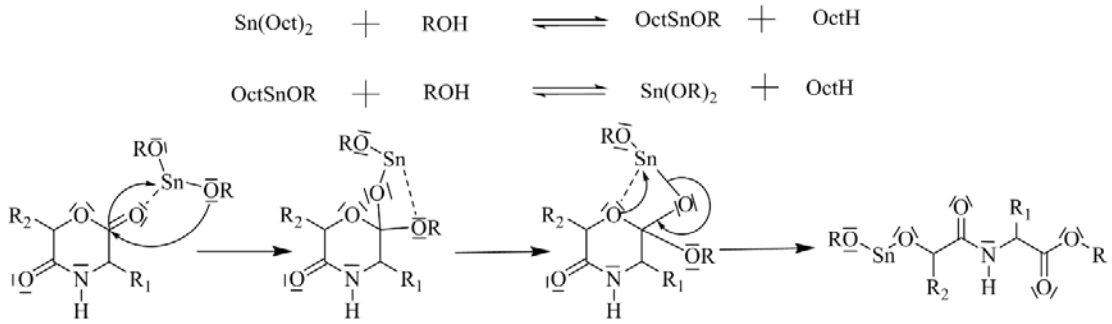

	R_1	R_2
(3S,6S)-3-isopropyl-6-methyl-2,5-morpholinedione	(3S)-isopropyl	(6S)-methyl
(6R,S)-6-methyl-2,5-morpholinedione	H	(6R,S)-methyl
(3S)-3-methyl-2,5-morpholinedione	(3S)-methyl	H
(3S)-3-isopropyl-2,5-morpholinedione	(3S)-isopropyl	H

Scheme 1. Coordination insertion mechanism of ROP of MDs catalyzed by $Sn(Oct)_2$ [11, 15].

We hypothesized that introducing pendant bulky groups into the MD would lower the T_g. Our strategy to achieve such a new class of MDs was to introduce a pendant alkyl group at the position 6 by a variation of the α-hydroxy acid part of the MDs to explore the effect of such a MD on the thermal properties of the final oligomer. Nevertheless, modifications at position 6 might influence the steric hindrance and decrease the efficiency of ROP [16]. Therefore, initial kinetic studies were

performed to compare the efficiency of the ROP of the two monomers modified at position 3 and 6, named (3R,S)-hexylmorpholine-2,5-dione (3HMD) and (3S, 6R,S)-3-methyl-6-hexylmorpholine-2,5-dione (3M6HMD). Furthermore, ROP of (3S)-methylmorpholine-2,5-diones (MMD) was performed as a reference ROP. The introduction of the atactic bulky side group would hinder the H-bond interactions resulting in a less regular structure, reduced the content of the crystalline phase, and lower T_gs of oligo3M6HMD (o3M6HMD) and oligo3HMD (o3HMD). After the detailed characterization of the synthesized MDs, the ROP kinetics were studied, and thermal properties of the resulting oDPs were explored.

Experimental

Materials

If not mentioned otherwise, catalyst and solvents were obtained from Sigma Aldrich (Seelze, Germany) and used as received. 2-Bromooctanoic acid (98%) was purchased from Th. Geyer (Hamburg, Germany), thionyl chloride (97%) and L-alanine were obtained from Roth (Karlsruhe, Germany). Tin(II) 2-ethylhexanoate ($Sn(Oct)_2$) was distilled three times before usage. Ethylene glycol (≥ 99%) was dried by stirring over $MgSO_4$, then distilled under inert conditions, and finally stored above molecular sieves. Solvents were dried by standard methods and distilled prior to usage.

Methods

Nuclear Magnetic Resonance (NMR) spectra were recorded on a Bruker DCX-500 spectrometer at room temperature (r.t.). In most cases DMSO-d_6 was used as deuterated solvent, 2-aminooctanoic acid was dissolved in D_2O/NaOD. The protonated species of the deuterated solvent

was used as an internal standard. Chemical shifts were referenced to DMSO-d_6 = 2.5 ppm and D_2O = 4.8 ppm, respectively.

The thermal properties of the polymers were determined by differential scanning calorimetry (DSC) on a Netzsch DSC 204 (Selb, Germany), which was equipped with a low-temperature cell. The cyclic measurements were conducted in the temperature range between -20 °C and 200 °C with a heating rate of 10 °C·min^{-1} and kept at 200 °C for 2 min. Subsequently, the sample was cooled with the same rate by liquid nitrogen. After 2 min at the lowest temperature, a second heating run was performed. The thermal transitions were evaluated from the second heating run.

Gel permeation chromatography (GPC) measurements were performed by universal calibration (see Supporting Information) on a system consisting of a precolumn, (two 300*8 mm^2 linear M (10 µ) SDV-columns, PSS = Polymer Standards Service GmbH, Mainz, Germany), a degasser DG-2080-53, a RI-1530 refractive index detector, an isocratic pump PU-1580, an automatic injector AS-1555 (all JASCO, Groß-Umstadt, Germany) and a viscosimeter T-60A detector (VISCOTEK, Houston TX, USA). Tetrahydrofuran (THF) was used as eluent at a flow rate of 1.0 mL·min^{-1} at r.t. and 0.2 wt% methanol as internal standard. Molecular weight and polydispersity calculations (see Supporting Information Figure S1 and S2 for GPC traces of samples listed in table 1 and 2, respectively) were performed using WINGPC 6.2 (PSS) SEC software (Polymer Standard Service, Mainz, Germany).

Matrix-assisted laser desorption/ionization time-of-flight mass spectroscopy (MALDI-TOF MS) was performed on a Biflex III spectrometer (Bruker Daltonik, Leipzig, Germnay). The samples were prepared as follows: 0.5 mg of the oligomer was dissolved in 1 mL THF, a mixture of *trans*-2-[3-(4-*tert*-butylphenyl)-2-methyl-2-propenylidene]malononitrile (DCTB) and potassium

trifluoroacetate in THF was used as matrix. High-resolution mass spectrometry (HRMS) was recorded on an ESI-Q-TOF maXis mass spectrometer (Bruker Daltonik, Leipzig, Germnay).
IR spectra were obtained using Magna IR 550 series II spectrometer (Nicolet, Germany), which was equipped with a single beam diamond ATR unit. Melting points were determined on an electrothermal MEL-TEMP (Bibby Sterilin, Stone, UK) apparatus at a starting temperature of 90 °C and a heating rate of 0.1 °C·min^{-1}.

Synthesis of monomers

Both monomers, 3HMD and 3M6HMD, were synthesized in a three-step synthesis route according to the procedure described in reference [17]. In brief, in a first step the N-(halogenacyl)amino acid was synthesized as an intermediate. Afterwards, the ring-closure reaction to the morpholine-2,5-dione was conducted. The overall yields for 3M6HMD and 3HMD were 15% and 7%, respectively.

*Synthesis of (2S)-2-(2-bromooctanamido)propanoic acid **3***

Thionyl chloride (3.1 g, 13.04 mmol) was added dropwise into a 50 mL Schlenk flask containing 2-bromooctanoic acid (2.5 g, 11.3 mmol), which was kept at 0 °C. The mixture was heated to 90 °C and refluxed at this temperature for 24 h. The acylation reaction was monitored by NMR spectroscopy until no signals from residual acid moieties could be observed. The excess of thionyl chloride was removed by vacuum at ambient temperature.
1.18 g (13.19 mmol) L-alanine was dissolved in 15 mL NaOH solution (1 M) and cooled by an ice bath (0 °C). The 2-bromooctanoyl chloride was dissolved in diethyl ether (16.8 mL) and added to the amino acid solution within 7 h simultaneously with 14 mL NaOH solution (1 M) under vigorous stirring. The pH was held at pH = 12 during the procedure. When the aqueous phase was

acidified to a pH of 3, a colorless precipitate was formed, which was filtered off, washed with hexane, and dried at 45 °C until constant weight was achieved.

^{1}H NMR (500 MHz, DMSO-d_6): δ ppm 12.60 (s, 1H, $CO_2\underline{H}$), 8.56 (d, J = 7.3, 1H,N$\underline{H}$), 4.45 - 4.36 (m, 1H, NH-C$\underline{H}$CH$_3$-CO$_2$H), 4.29 - 4.14 (m, 1H; Br-C$\underline{H}$C$_6$H$_{13}$-CO), 1.97 - 1.52 (m, 2H, C$_5$H$_{11}$-C$\underline{H_2}$-CHBr), 1.52 - 1.00 (m, 11H; (C$\underline{H_2}$)$_4$-CH$_3$/NH-CHC$\underline{H}_3$-CO$_2$H), 0.85 (t, J = 6.8, 3H, (CH$_2$)$_5$-C$\underline{H_3}$); ^{13}C NMR (126 MHz, DMSO-d_6): δ ppm 173.3 ($\underline{C}$O$_2$H), 167.9 (CHBr-$\underline{C}$O-NH), 48.5 (Br-$\underline{C}$HC$_6$H$_{13}$-CO), 47.6 (NH-$\underline{C}$HCH$_3$-CO$_2$H), 34.4 (C$_5$H$_{11}$-$\underline{C}$H$_2$-CHBr), 30.7 (C$_2$H$_5$-$\underline{C}$H$_2$-CH$_2$), 27.6 (C$_3$H$_7$-$\underline{C}$H$_2$-CH$_2$), 26.3 (C$_4$H$_9$-$\underline{C}$H$_2$-CH$_2$), 21.6 (CH$_3$-$\underline{C}$H$_2$-CH$_2$), 16.9 (NH-CH$\underline{C}$H$_3$-CO$_2$H), 13.6 ((CH$_2$)$_5$-$\underline{C}$H$_3$); MS (ESI$^+$): [M$_{H^+}$]$_{determined}$ 294.0714, [M]$_{theoretical}$ 293.0705; melting point: 85 ± 2 °C.

Synthesis of (3S,6R,S)-3-methyl-6-hexylmorpholine-2,5-dione (3M6HMD) ***4***

0.50 g (1.7 mmol) of ***3*** and triethylamine (TEA) (0.5 g, 4.82 mmol) were mixed homogeneously in DMF (75 mL) under vigorous stirring. The reactor was heated to 60 °C and kept at this temperature for 3 h, then cooled to r.t. and kept at r.t. for another 24 h. The precipitate, triethylamine hydrobromide, was filtered off and the obtained solution was filtered over silica gel. After removal of the solvent under vacuum, recrystallization from ethyl acetate for two times gave colorless crystals. The overall yield was 15%.

^{1}H NMR (500 MHz, DMSO-d_6): δ ppm 8.49 (s, 1H; N$\underline{H}$), 4.96 (dd, J = 7.7, 1H; O-C$\underline{H}$(C$_6$H$_{11}$)-CO), 4.46 - 4.28 (m, 1H; NH-CHCH$_3$-CO), 1.94 - 1.63 (m, 2H, C$_5$H$_{11}$-C$\underline{H_2}$-CH), 1.47 - 1.18 (m, 11H, (C$\underline{H_2}$)$_4$-CH$_3$/NH-CHC$\underline{H}_3$-CO), 0.87 (t, J = 6.8, 3H; (CH$_2$)$_5$-C$\underline{H_3}$); ^{13}C NMR (126 MHz, DMSO-d_6): δ ppm 170.6 (CHC$_6$H$_{13}$-$\underline{C}$O-NH), 168.6 (CHCH$_3$-$\underline{C}$O-O), 77.5 (O-$\underline{C}$HC$_6$H$_{13}$-CO), 48.6 (NH-$\underline{C}$HCH$_3$-CO), 31.4 (C$_5$H$_{11}$-$\underline{C}$H$_2$-CH), 29.6 (C$_2$H$_5$-$\underline{C}$H$_2$-CH$_2$), 28.7 (C$_3$H$_7$-$\underline{C}$H$_2$-CH$_2$), 24.5 (C$_4$H$_9$-$\underline{C}$H$_2$-CH$_2$), 22.3 (CH$_3$-$\underline{C}$H$_2$-CH$_2$), 16.2 (NH-CH$\underline{C}$H$_3$-CO), 14.2 ((CH$_2$)$_5$-$\underline{C}$H$_3$); IR

(ATR): 3199, 2922, 1749, 1693, 1530 cm^{-1}; MS (ESI^+): $[M_{H^+}]_{determined}$ 214.1447, $[M]_{theoretical}$ 213.1443; melting point: 117 ± 2 °C.

*Synthesis of 2-aminooctanoic acid **5***

In a 100 mL round-bottomed flask, 2-bromooctanoic acid (5 g, 22.6 mmol), sodium azide (3.6 g, 55 mmol), and 50 mL of DMSO were mixed homogeneously by stirring at 80 °C for 72 h. Then the solvent was removed by application of vacuum whereby the NaBr precipitated. After dissolving the residue in 30 mL dichloromethane (DCM), the precipitate was filtered off. Afterwards, the remaining solution was extracted several times with water. The organic phase was dried overnight over sodium sulfate. Once the sodium sulfate was filtered off, a yellow solution was obtained, which was used without further purification.

In a 1 L round flask, 10% palladium on carbon (100 mg) was added into the yellow solution and the mixture was vigorously stirred under a H_2 atmosphere. Once a colorless solid precipitated, additional palladium on carbon (30 mg) and DCM were added. Hydrogenation was continued for another 48 h. Afterwards, the residual solvent was decanted. Extraction with boiling water and ethanol for three times gave colorless crystals, which were further dried in an oven at 45 °C until constant weight was achieved.

^{1}H NMR (500 MHz, D_2O/NaOD): δ ppm 3.20 (dd, *J* = 7.0, 1H,CO_2H-C*H*C_6H_{13}-N*H*$_2$), 1.65 - 1.46 (m, 2H, C_5H_{11}-C*H*$_2$-CH), 1.38 - 1.22 (m, 8H, (C*H*$_2$)$_4$-CH_3), 0.92 - 0.81 (m, 1H, $(CH_2)_4$-C*H*$_3$),; ^{13}C NMR (126 MHz, D_2O/NaOD): δ ppm 181.2 (*C*O_2H), 53.3 (CO_2H-*C*HC_6H_{13}-N*H*$_2$), 32.0 (C_5H_{11}-*C*H_2-CH), 28.2 (C_2H_5-*C*H_2-CH_2), 25.7 (C_3H_7-*C*H_2-CH_2), 22.2 (C_4H_9-*C*H_2-CH_2), 19.2 (CH_3-*C*H_2-CH_2), 10.6 ($(CH_2)_5$-*C*H_3); MS (ESI^+): $[M_{H^+}]_{determined}$ 160.1336, $[M]_{theoretical}$ 159.1336; melting point: 268 ± 2 °C.

*Synthesis of 2-(2-chloroacetamido)octanoic acid **6***

3 g (19 mmol) of ***5*** was dissolved in 20 mL NaOH solution (1M) and cooled by an ice bath (0 °C). 2-chloroacetyl chloride (20 mmol) was dissolved in diethyl ether (20 mL) and added to the amino acid solution within 7 h whereby 20 mL NaOH solution (1 M) was added simultaneously under vigorous stirring. The pH was held at pH = 12 during the procedure. Afterwards, acidification of the aqueous phase with HCl resulted in a colorless solid precipitate. The precipitate was filtered off, extracted with hexane, and dried overnight at 45 °C until constant weight was achieved. ^{1}H NMR (500 MHz, DMSO-d_6): δ ppm 12.68 (s, 1H, $CO_2\underline{H}$), 8.44 (d, J = 7.8, 1H, N$\underline{H}$), 4.18 (td, J = 8.3, 1H, NH-C$\underline{H}C_6H_{13}$-CO), 4.10 (m, 2H, Cl-C$\underline{H_2}$-CO), 1.65 (m, 2H, C_5H_{11}-C$\underline{H_2}$-CH), 1.25 (m, 8H, (C$\underline{H_2}$)$_4$-CH_3), 0.85 (t, J = 6.8, 3H, $(CH_2)_4$-C$\underline{H_3}$); ^{13}C NMR (126 MHz, DMSO-d_6): δ ppm 173.4 ($CO_2\underline{H}$), 166.1 (CH_2Cl-$\underline{C}$O-NH), 52.3 (NH-$\underline{C}HC_6H_{13}$-CO), 42.5 (Cl-$\underline{C}H_2$-CO), 31.2 (C_5H_{11}-$\underline{C}H_2$-CH), 31.1 (C_2H_5-$\underline{C}H_2$-CH_2), 28.3 (C_3H_7-$\underline{C}H_2$-CH_2), 25.3 (C_4H_9-$\underline{C}H_2$-CH_2), 22.1 (CH_3-$\underline{C}H_2$-CH_2), 14.1 ($(CH_2)_5$-$\underline{C}H_3$); MS (ESI$^+$): $[M_{H^+}]_{determined}$ 236.1055, $[M]_{theoretical}$ 235.1053; melting point: 87 ± 1 °C.

*Synthesis of (3R,S)-hexylmorpholine-2,5-dione (3HMD) **7***

1.00 g (4.3 mmol) of ***6*** and TEA (1.0 g, 5.64 mmol) were mixed homogeneously in DMF (150 mL) under vigorous stirring. The reactor was heated to 60 °C, kept at this temperature for 3 h, then cooled to r.t. and kept at this temperature for another 24 h. After removal of triethyl hydrochloride and passing through silica gel, the solvent was decanted. Recrystallization from ethyl acetate for two times gave white crystals. The overall yield was 7%.

^{1}H NMR (500 MHz, DMSO-d_6): δ ppm 8.56 (s, 1H, N<u>*H*</u>), 4.73 (q, 2H, O-C<u>*H*</u>$_2$-CO), 4.16 (td, *J* = 6.0, 1H, NH-C<u>*H*</u>C$_6$H$_{13}$-CO), 1.73 (m, 2H, C$_5$H$_{11}$-<u>*C*</u>H2-CH), 1.32 (m, 8H; (C<u>*H*</u>$_2$)$_4$-CH$_3$), 0.86 (t, *J* = 6.8, 3H; -(CH$_2$)$_4$-C<u>*H*</u>$_3$); ^{13}C NMR (126 MHz, DMSO-d_6): δ ppm 168.1 (CH$_2$-<u>*C*</u>O-NH), 165.5 (CHC$_6$H$_{13}$-<u>*C*</u>O-O), 67.2 (O-<u>*C*</u>H$_2$-CO), 52.0 (NH-<u>*C*</u>HC$_6$H$_{13}$-CO), 31.1 (C$_5$H$_{11}$-<u>*C*</u>H$_2$-CH), 30.7 (C$_2$H$_5$-<u>*C*</u>H$_2$-CH$_2$), 27.9 (C$_3$H$_7$-<u>*C*</u>H$_2$-CH$_2$), 23.9 (C$_4$H$_9$-<u>*C*</u>H$_2$-CH$_2$), 21.7 (CH$_3$-<u>*C*</u>H$_2$-CH$_2$), 13.6 ((CH$_2$)$_5$-<u>*C*</u>H$_3$); IR (ATR): 3196, 2914, 1740, 1691, 1546 cm^{-1}; MS (ESI$^+$): $[M_H{}^+]_{determined}$ 199.1205, $[M]_{theoretical}$ 199.1208; melting point: 100 ± 2 °C.

Synthesis of (3S)-methylmorpholine-2,5-diones (MMD)

The synthesis of (3S)-methylmorpholine-2,5-diones was performed according to the synthesis route described in reference [18].

^{1}H NMR (500 MHz, DMSO-d_6): δ(ppm) 8.53 (s, 1H, N<u>*H*</u>), 4.92 - 4.54 (q, 2H, O-C<u>*H*</u>$_2$-CO), 4.30 (q, 1H, NH-C<u>*H*</u>CH$_3$-CO), 1.33 (d, 3H, CHC<u>*H*</u>$_3$). melting point: 138 ± 1 °C.

Synthesis of oDPs

oDPs were synthesized by ROP of the morpholine-2,5-dione (MD) as shown in Scheme 2.

A general procedure was based on polymerization of MDs catalyzed by Sn(Oct)$_2$ using ethylene glycol (EG) as initiator. Polymerization reactions were carried out with approximate 1 g monomer (n_{MMD} = 7.8 mmol; n_{3M6HMD} = 4.7 mmol; n_{3HMD} = 5.0 mmol, respectively). Monomer, predefined amount of initiator, and catalyst were filled into a flame-dried Schlenk reactor (10 mL) under a dry nitrogen atmosphere. Afterwards, the reaction mixture was heated to the polymerization temperature and stirred under inert conditions for time periods according to Table 1and 2. The targeted molecular weights for oDPs were 6 kg·mol^{-1}.

The ROP kinetics were studied at 140 °C. Samples were taken at appropriate time intervals and the ROP was quenched by freezing in liquid nitrogen. Afterwards, the crude samples were directly analyzed by GPC measurements without any further purification and removal of unreacted monomer. The monomer conversions were determined from GPC eluograms via comparing the integrals from monomer peaks with the sum of integrals of the peaks from monomers and oligomers.

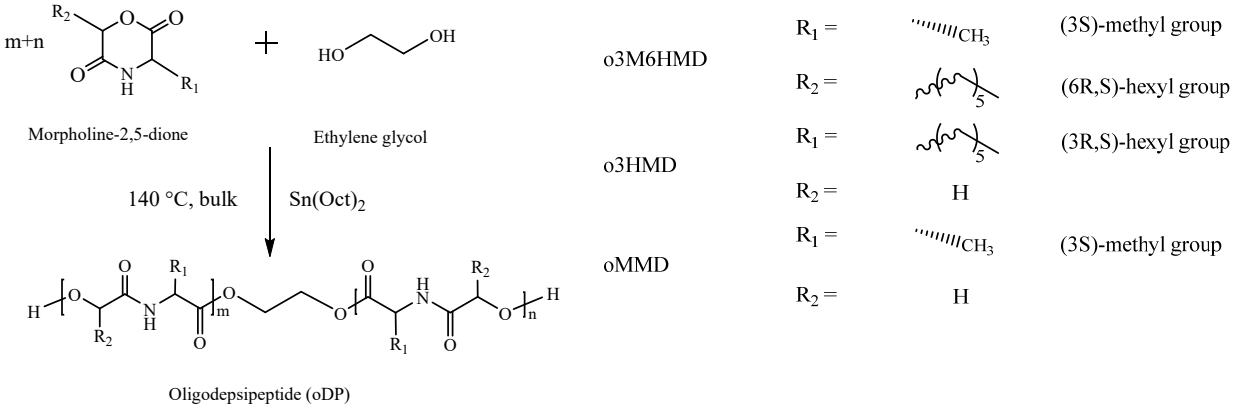

Scheme 2. ROP of morpholine-2,5-diones.

Results and discussion

Monomer synthesis

In general, monomers were synthesized in a three-step synthesis route according to scheme 3. 2-bromooctanoic acid was transferred to 2-Bromooctanoyl chloride as well as to 2-aminooctanoic acid to create related acetyl chloride in case of 3M6HMD and the α-amino acid in case of 3HMD. The related α-amino acid was reacted with the appropriate acyl halide in a modified Schotten-Baumann reaction at the interphase between diethyl ether and water. The presence of NaOH in the aqueous phase neutralizes the generated carboxylic acid and shifts in this way the equilibrium

reaction to the corresponding intermediate products. The monomers (3M6HMD and 3HMD), which were created in a subsequently performed ring-closure reaction, were purified by recrystallization from ethyl acetate. Stuctures of all synthesized compounds were confirmed by ^{1}H NMR and ^{13}C NMR spectroscopy as well as mass spectrometry.

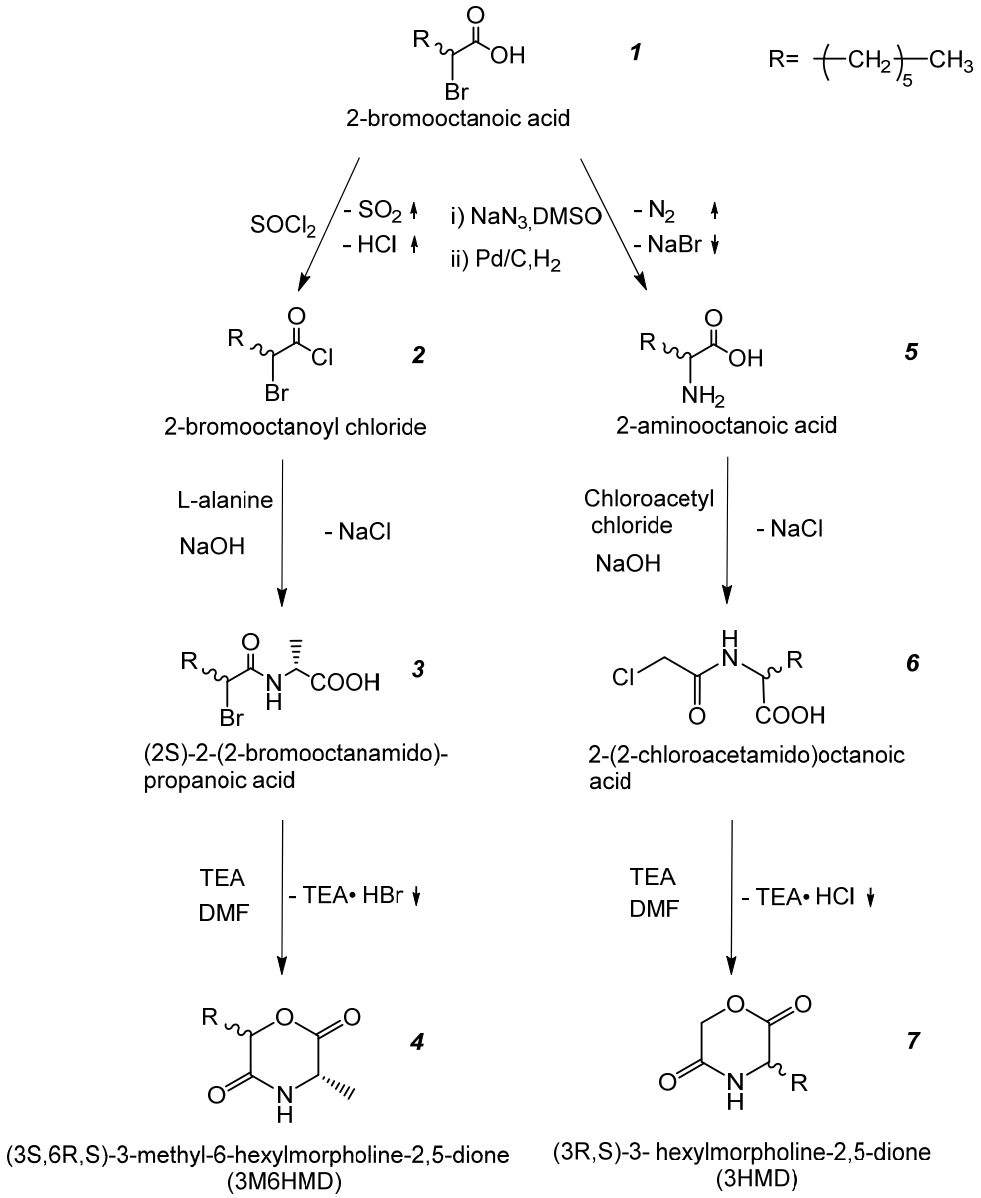

Scheme 3. Synthesis of morpholine-2,5-diones.

Table 1. Comparision of ROP of MMD and 3M6HMD catalysed by $Sn(Oct)_2$.

Run	Monomer	$[M]_0:[EG]_0:[Sn(Oct)_2]_0$[a]	ROP condition	Time [h]	$M_{n,GPC}$[b] [kg·mol^{-1}]	M_w/M_n	Conversion[c] [%]
1	3M6HMD	500:18:1	Toluene 80 °C[d]	3	n.d[e]	n.d	7
2	3M6HMD	500:18:1	Toluene 110 °C[d]	3	n.d	n.d	21
3	3M6HMD	500:18:1	Bulk 140 °C	3	3.2	1.1	36
4	3M6HMD	500:18:1	Bulk 140 °C	15	4.8	1.2	49
5	MMD	500:11:1	Toluene 80 °C[d]	3	n.d	n.d	15
6	MMD	500:11:1	Toluene 110 °C[d]	3	n.d	n.d	29
7	MMD	500:11:1	Bulk 140 °C	3	4.3	1.1	47
8	MMD	500:11:1	Bulk 140 °C	15	5.3	1.4	83
9[f]	3M6HMD	500:18:1	Bulk 140 °C	24	4.3	1.6	49
10[f]	MMD	500:11:1	Bulk 140 °C	24	5.6	1.2	83
11[f]	3HMD	500:17:1	Bulk 140 °C	24	5.4	1.3	79

[a] M_n of oligomers was aimed at 6 kg·mol^{-1}.
[b] M_n was determined by GPC using THF as an eluent.
[c] Monomer conversion was determined by GPC using THF as an eluent.
[d] Monomer concentration was 0.94 mol·L^{-1}.
[e] n.d : no data.
[f] Polymerizations were performed for kinetic study, see Figure 1.

Determination of reaction parameters by ROP of 3M6HMD

The capability of the newly created compounds acting as monomers in ROP was explored in preliminary homopolymerizations catalyzed by $Sn(Oct)_2$. In a feasibility study, the optimum reaction conditions for the ROP were determined by ROP of MMD. These optimized parameters were used for ROP of 3M6HMD. In this way, the influence of modification at position 6 was investigated. The efficiency of the reactions was evaluated by determining the monomer conversions after appropriate time intervals (Table 1). In initial experiments, ROP was conducted in solution (toluene) and at 80 °C to avoid side reactions. The monomer conversions with 7% and

15% were relatively low after 3 h at 80 °C for both 3M6HMD and MMD, respectively. A slight increase of monomer conversion was achieved when the temperature was raised from 80 °C to 110 °C. The monomer conversion increased tremendously when the ROP was performed as bulk polymerization of the melt at 140 °C. In case of 3M6HMD conversions of 36% and 49% were achieved after 3 h and 15 h. When MMD was polymerized, the conversion increased to 47% after 3 h and to 83% after 15 h at the same conditions. The difference in the monomer conversions between 3M6HMD and MMD might be attributed to the steric hindrance caused by hexyl group substitute.

Kinetic study of ROP

In the ROP kinetic study experiments of 3M6HMD, 3HMD, and MMD (Table 1, runs 9-11), the polymerizations were catalyzed by $Sn(Oct)_2$. Samples were collected from the reaction mixture, dissolved in THF, and analyzed by GPC.

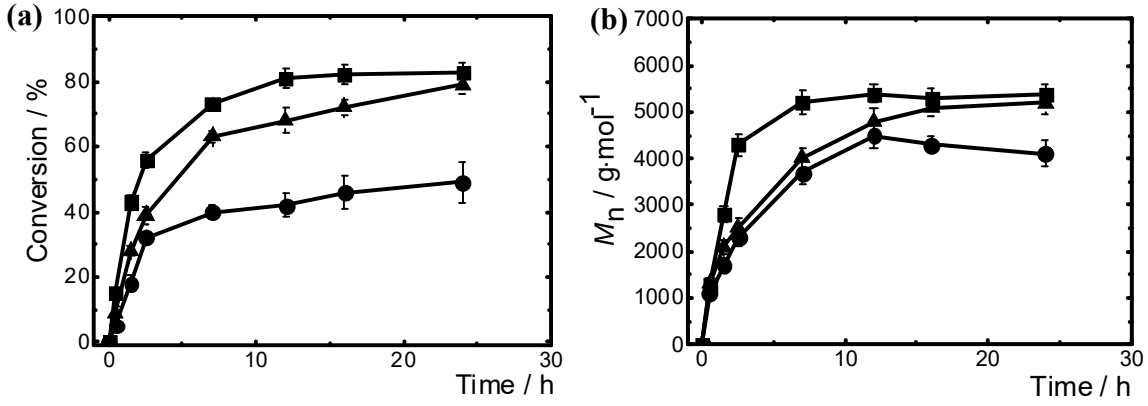

Figure 1. Homopolymerization of MDs catalyzed by $Sn(Oct)_2$: (a) dependence of monomer conversion on time; (b) dependence of M_n on time. MMD ■; 3M6HMD ●; 3HMD ▲.

Figure 1a displays the dependence of the monomer conversion as a function of time. MMD achieved the highest monomer conversion at any given time during the reaction, which indicates that MMD have the highest activity towards the ROP. The ring-chain equilibria were reached for both MMD and 3M6HMD after 12 h, while a slight increase was still observed for 3HMD after 16 h. When the reactions reached the equilibria, 3M6HMD displayed the lowest monomer conversion of around 50% among the three monomers in the given reaction conditions. In contrast, MMD and 3HMD presented a reasonable conversion of around 80% after 24 h. The obtained results show clearly the differences in the reactivity of each monomer in the ROP, which is supposed to be caused by the steric hindrance of the hexyl group substitute.

Figure 1b presents the obtained M_n as a function of the reaction time. A similar tendency of increase as observed for the conversion can be noted. The highest M_n was observed for ROP of MMD. After 12 h and 16 h of the reaction time, almost constant M_ns were reached for MMD and 3HMD, respectively. In case of 3M6HMD, the M_n decreased after reaching a maximum value after 12 h. Due to the presence of the hexyl group at position 6 in the 3M6HMD, the efficiency of ROP should be relatively low, which was also observed in a kinetic study. The decrease of M_n, as presented in Figure 1b, after reaching the maximum value indicates that the intermolecular side reactions became the favored reaction versus the competing chain growth reaction. Analogous observations were reported by former research work on ROP of morpholine-2,5-diones [15]. The decrease of M_n was attributed to the chain fragmentation reaction, which means that the polymer chains were partially transferred to the $Sn(Oct)_2$ via intermolecular transesterification resulting in polymer chains terminated with tin residue. Meanwhile, back-biting leading to macrocycle can also contribute to the reduction of M_n via intramolecular transesterification, which can be confirmed by MALDI-TOF (Figs. 4-6).

Figure 2 shows the kinetic plots of the polymerization of the monomers in semilogarithmic scale. The time law for polymerization with ring-chain equilibrium can be expressed according to equation (1)[19, 20]:

$$ln\frac{M_0 - M_e}{M_t - M_e} = K_p[Cat][M]^* t = K_{app} t \quad (1)$$

M_0 is the monomer concentration of the starting mixture, M_e represents the monomer concentration at the moment when reaction reaches the ring-chain equilibrium, M_t is the determined monomer concentration after various reaction time periods, and M^* is the concentration of the active species. The slope of the plot is the apparent rate constant K_{app} ($K_{app} = K_p[Cat][M]^*$), which is a direct parameter for the reaction rate at the given reaction conditions.

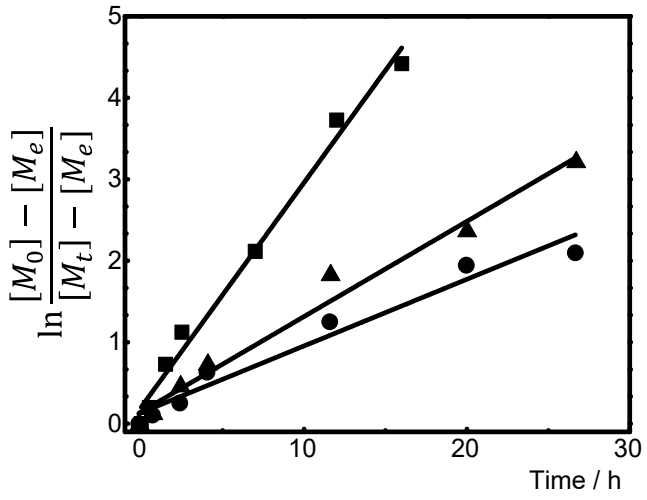

Figure 2. Homopolymerization of MDs in bulk catalyzed $Sn(Oct)_2$: 1st order plot. MMD ■; 3M6HMD ●; 3HMD ▲.

The monomer reaction activities for the ROP are comparable to the apparent rate constants K_{app}s obtained from the slopes of the semilogarithmic-time curves. In case of MMD the rate constant obtained a value of 0.28 ± 0.01 h^{-1}, which is 2 times higher than for the ROP of 3M6HMD with a rate constant of 0.14 ± 0.02 h^{-1}. This can be attributed to the steric hindrance introduced by hexyl-

group substitute at position 6. The rate constant of ROP of 3HMD was 0.20 ± 0.03 h^{-1}. This lower K_{app} compared to ROP of MMD can also be explained by the steric hindrance caused by the substitution of methyl group with the hexyl group at position 3. Compared with 3M6HMD, the higher K_{app} of 3HMD can be explained by a slight electron pushing effect (+I-effect) of the hexyl group compared to the hydrogen in addition to the steric hindrance.

In general, the amide group of depsipeptide is considered to be more stable than an ester group and less active towards ROP. However, attempts to synthesize polydepsipeptides from the corresponding N-alkyl substituted morpholine-2,5-diones via ROP have not been successful until now [21]. A possible explanation might be that the amide group could form a chelating intermediate at the ester group. In this context, the reduction of the monomer activity for ROP in case of 3HMD, could be caused by the steric hindrance introduced by hexyl-substitute at position 3.

Investigation of MDs homopolymerization

The homopolymerization of MDs was studied by ROP. The reactions were quenched after appropriate time periods before intermolecular side reactions became the favored reactions. The obtained oligomers were characterized by NMR, GPC, MALDI-TOF, and DSC (see Supporting Information Figure S3 for full MALDI-TOF spectra of o3M6HMD and o3HMD, Figure S4 for DSC curves, and Figure S5 for ^{13}C NMR spectra of o3M6HMD and o3HMD).

Table 2. ROP of MMD, 3M6HMD, and 3HMD at 140 °C in melt catalyzed by $Sn(Oct)_2$

Monomer	$[M]_0$:$[EG]_0$:$[Sn(Oct)_2]_0$[a] (equiv.)	Reaction Time[c][h]	Yield [%]	DP Aimed[d]	DP Measured[e]	M_n [kg·mol^{-1}] NMR	M_n [kg·mol^{-1}] GPC	M_w/M_n
MMD	500:11:1	16	62	46	44	6.5 ± 0.3	5.7 ± 0.6	1.4
3M6HMD[b]	500:18:1	12	23	28	25	6.1 ± 0.3	5.4 ± 0.5	1.2
3HMD[b]	500:17:1	18	58	30	28	5.8 ± 0.3	5.6 ± 0.6	1.2

[a] M_n of oligomers was 6 kg·mol^{-1}.
[b] Purified by chromatography.
[c] Reaction time periods were defined with contribution of the results from kinetic study.
[d] Aimed degree of polymerization (DP) was based on the molar ratio of starting compounds.
[e] Determined by GPC on the purified product.

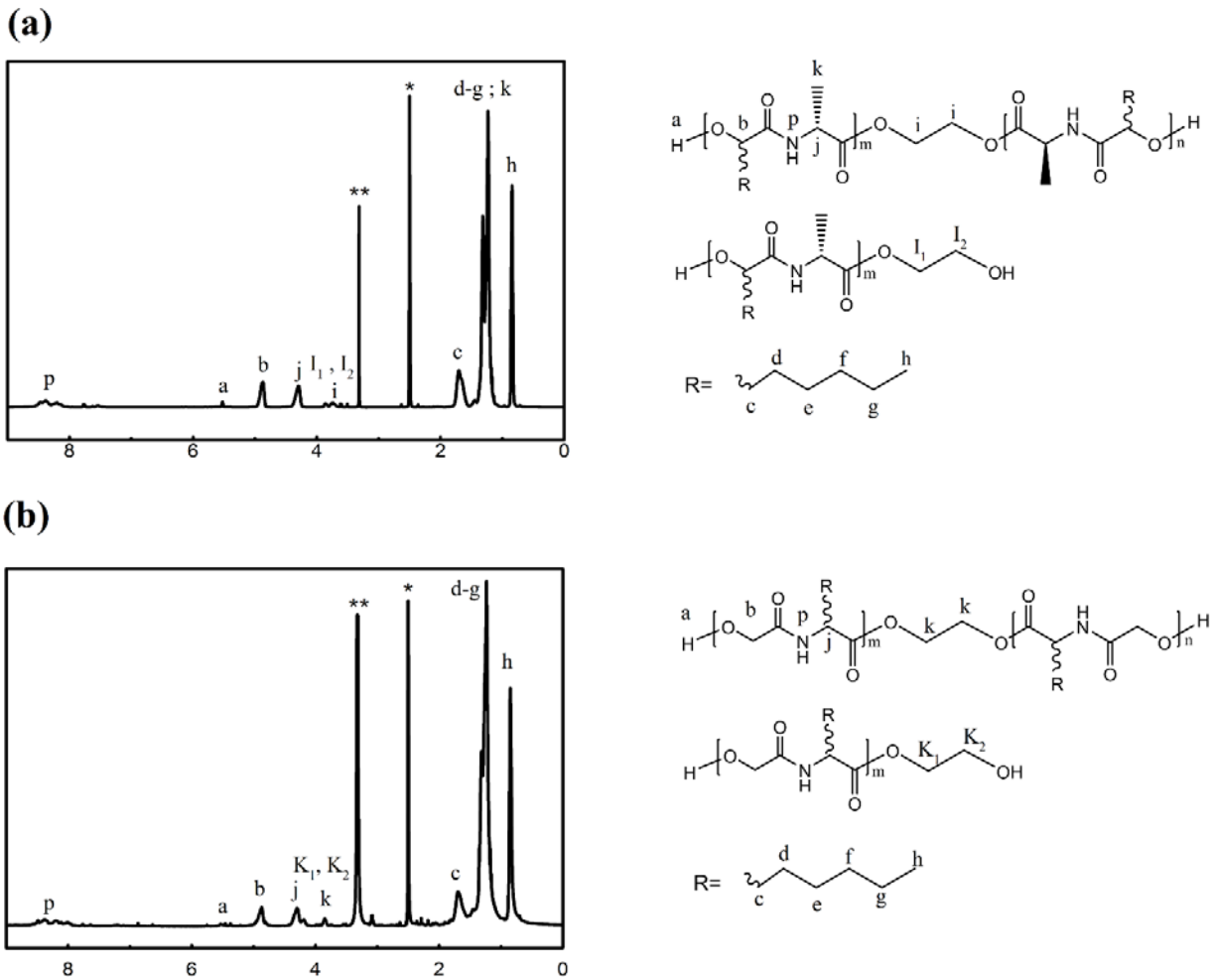

Figure 3. 500 MHz ^{1}H NMR spectra in DMSO-d_6 of (a) o3M6HMD and (b) o3HMD. One asterisk indicates the DMSO peak, and two asterisks indicate the H_2O peak.

When the molecular weights of the oligomers were determined by ^{1}H NMR, the ratio of the signal intensities of the repeating units and initiator were calculated according to equation (2):

$$M_n = \frac{I_{CH_3}/3}{I_{CH_2}/4} * M_{morpholine\ dione} + M_{Initiator} \quad (2)$$

I_{CH_3} and I_{CH_2} are integrals of the signals originating from the initiator at δ = 3.80 - 3.88 ppm and from the oDPs repeating unit at δ = 0.76 - 0.89 ppm for o3M6HMD and at δ = 0.68 - 0.91 ppm for o3HMD (shown in Figure 3a and Figure 3b).

The molecular masses of the oDPs were also determined by GPC and the data are summarized in Table 2. The M_w/M_n of oMMD was 1.4, which was slightly higher than 1.2 of o3M6HMD and o3HMD. This slightly higher value can be explained by a lower solubility of the oligomer in the melted monomer resulting in precipitation and by this in a loss of control of the polymerization reaction.

MALDI-TOF MS was performed on o3M6HMD and o3HMD to characterize the terminal groups of the obtained oligomers (Figure 4). Four series of signals corresponding to three different species could be identified for the telechelic o3M6HMD as shown in Figure 4a. The main series 2 and 2′corresponding to the oligomers are the series with terminal hydroxyl groups having 7 or 8 repeating units, respectively. Series 1 represents the polymer chain ionized by accidentally introduced sodium ions. Series 3 can be attributed to the formation of macrocycles by intramolecular transesterification. The molar mass of series 4 is 44 g·mol^{-1} less than the molar mass of series 2′ and results from the polymer chains providing carboxylic terminal groups, which were initiated by traces of water or other active hydroxyl-containing species in the starting mixture.

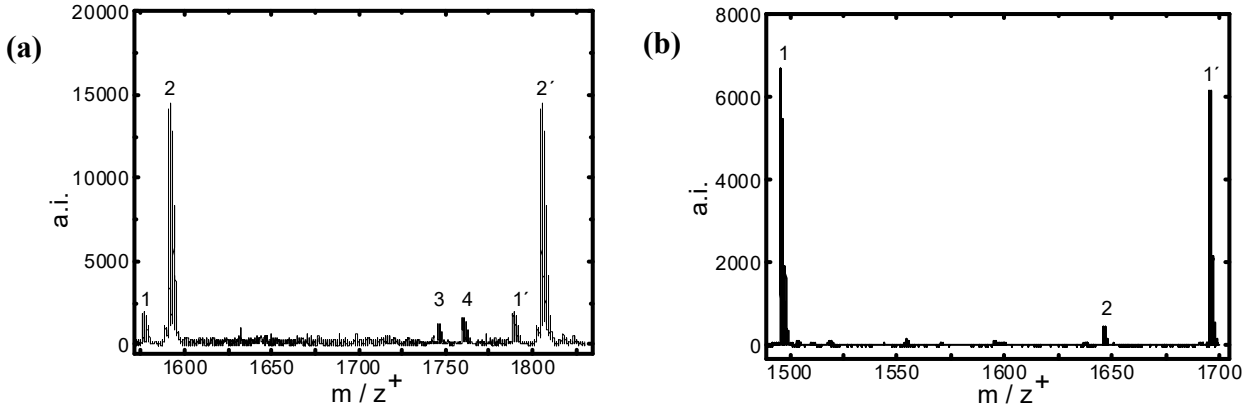

Figure 4. Details of MALDI-TOF mass spectra, reflector negative ion mode: (a) o3M6HMD and (b) o3HMD.

The structures of the corresponding species identified from the o3M6HMD mass spectrum are presented in Figure 5. A lower number of signal series can be observed compared to the spectra of o3M6HMD in the MALDI-TOF spectrum of o3HMD (Figure 4b). Series 1 and 1´ can be correlated to oligomers with repeating units 7 or 8. The structures of the corresponding species, which can be identified from the o3HMD MALDI-TOF mass spectra, are displayed in Figure 6. Series 2 is caused by water initiation as discussed before. The low content of additional series in the spectrum of o3HMD can be explained by higher activity of 3HMD towards the chain growth reaction, resulting in a better reaction control.

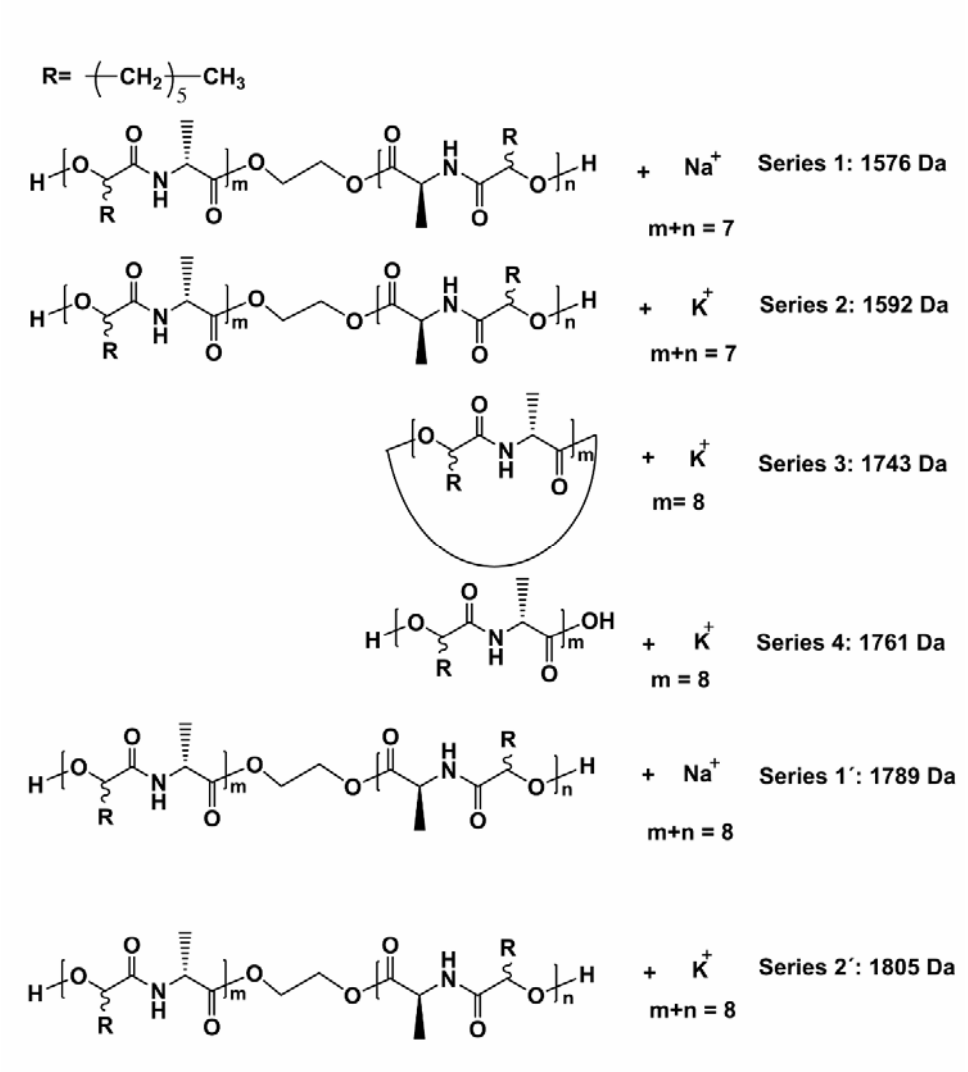

Figure 5. Structures of the species as assigned from the o3M6HMD mass spectrum.

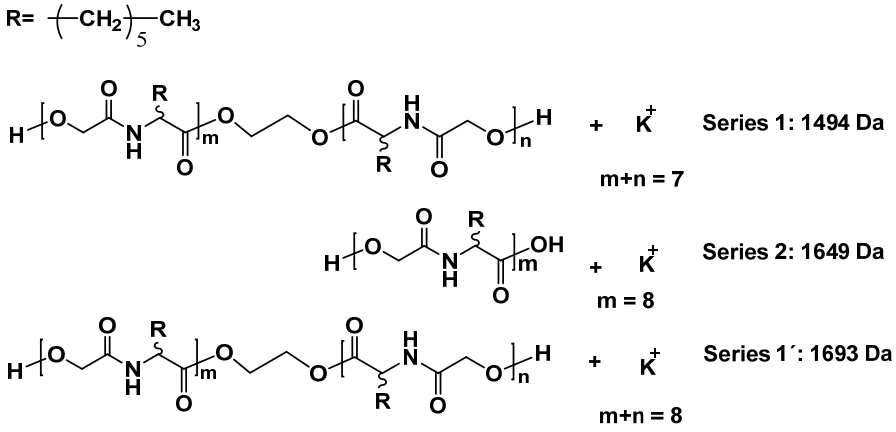

Figure 6. Structures of the species as assigned from the o3HMD mass spectrum.

In order to determine efficiency to reduce the glass transition temperature (T_g) by introducing atactic bulky side group, the thermal properties of oligomers with comparable molecular weights were studied by DSC (Table 3). The o3HMD exhibited the lowest T_g of 32 °C, which is below human body temperature. The o3M6HMD showed a close value of 36 °C around body temperature. In contrast, the T_g of oMMD was 65 °C, which is approximately 30 °C higher than the T_gs for both other oDPs in which hexyl side groups were introduced. This behavior could be caused by bulky atactic pendant groups, resulting in a plasticizing effect by disturbing the H-bonding between polymer chains. Meanwhile, the higher T_g. of oMMD can also be attributed to more polymer chains due to the lower monomer mass, which contributed a higher number of terminal hydroxy groups. As a result, the H-bonding was relatively enhanced leading to a stronger limitation of polymer chain movements. Furthermore, the absence of a second transition temperature (T_m) in both o3M6HMD and o3HMD strongly suggested amorphous polymers resulting in no significant crystalline domains. Both factors, the reduction of H-bonding and the weakening of crystalline behavior, could contribute to the enhancement of polymer chain movement.

Table 3 Thermal properties of synthesized oDPs

oDPs	T_g [°C]	T_m[a] [°C]
oMMD	65	142
o3M6HMD	36	n.d
o3HMD	32	n.d

[a] No T_m is detected in o3M6HMD and o3HMD

Conclusion

Two morpholine-2,5-diones, named 3M6HMD and 3HMD with atactic hexyl groups, were successfully synthesized via acylation reaction and subsequent ring-closure reaction. In initial studies, the ROP capability of 3M6HMD and 3HMD using ethylene glycol as initiator and $Sn(Oct)_2$ as coordination insertion catalyst was explored. In both oDPs no T_m could be detected suggesting the presence of only amorphous phases. The glass transition temperatures of o3M6HMD and o3HMD were approximately 30 °C lower than that of oMMD. All oligomers provided the presence of hydroxyl groups whereas in ROP of 3HMD less side reactions seemed to occur as evidenced by a lower number of series in MALDI-TOF measurements compared to that of o3M6HMD. K_{app} of 3M6HMD was slightly lower compared to 3HMD, which was a hint that in addition to the steric hindrance also the electron influence of the substitutions needs to be considered. Nevertheless, the oligomers from MDs providing terminal hydroxyl groups can be considered as valuable building blocks for degradable, elastic scaffold materials e.g. for cell culture systems.

Acknowledgments:

This work was financially supported by the Helmholtz-Association through programme-oriented funding, the Deutsche Forschungsgemeinschaft (DFG) through the Collaborative Research Centre 1112 “Nanocarriers”, subproject A03, the Tianjin University-Helmholtz-Zentrum Geesthacht, Joint Laboratory for Biomaterials and Regenerative Medicine, which is financed by the German Federal Ministry of Education and Research (BMBF, Grant No. 0315496) and the Chinese Ministry of Science and Technology (MOST, 2008DFA51170), and X.P. gratefully acknowledges funding by the China Scholarship Council (CSC) (grant No. 201206250098).

References

1. Ohya Y, Nakai T, Nagahama K, Ouchi T, Tanaka S, and Kato K. Journal of Bioactive and Compatible Polymers 2006;21(6):557-577.
2. Ohya Y, Matsunami H, Yamabe E, and Ouchi T. Journal of Biomedical Materials Research Part A 2003;65(1):79-88.
3. Abayasinghe NK, Perera KPU, Thomas C, Daly A, Suresh S, Burg K, Harrison GM, and Smith DW. Journal of Biomaterials Science, Polymer Edition 2004;15(5):595-606.
4. Ohya Y, Matsunami H, and Ouchi T. Journal of Biomaterials Science, Polymer Edition 2004;15(1):111-123.
5. Fonseca AC, Gil MH, and Simões PN. Progress in Polymer Science 2014;39(7):1291-1311.
6. Shi C, Yao F, Li Q, Khan M, Ren X, Feng Y, Huang J, and Zhang W. Biomaterials 2014;35(25):7133-7145.
7. Elomaa L, Kang Y, Seppälä JV, and Yang Y. Journal of Polymer Science Part A: Polymer Chemistry 2014;52(23):3307-3315.
8. Elomaa L, Pan C-C, Shanjani Y, Malkovskiy A, Seppälä JV, and Yang Y. Journal of Materials Chemistry B 2015;3(42):8348-8358.
9. Zhao Y, Li J, Yu H, Wang G, and Liu W. International Journal of Pharmaceutics 2012;430(1):282-291.
10. Feng Y, Lu W, Ren X, Liu W, Guo M, Ullah I, and Zhang W. Polymers 2016;8(2):13.
11. in 't Veld PJA, Dijkstra PJ, van Lochem JH, and Feijen J. Die Makromolekulare Chemie 1990;191(8):1813-1825.
12. Feng Y, Lu J, Behl M, and Lendlein A. Macromolecular Bioscience 2010;10(9):1008-1021.
13. Storey RF and Sherman JW. Macromolecules 2002;35(5):1504-1512.

14. Albertsson A-C and Varma IK. Biomacromolecules 2003;4(6):1466-1486.
15. Jörres V, Keul H, and Hoecker H. Macromolecular Chemistry and Physics 1998;199(5):835-843.
16. Küllmer K, Kikuchi H, Uyama H, and Kobayashi S. Macromolecular Rapid Communications 1998;19(2):127-130.
17. Barrera DA, Zylstra E, Lansbury PT, and Langer R. Macromolecules 1995;28(2):425-432.
18. Feng Y, Chen C, Zhang L, Tian H, and Yuan W. Transactions of Tianjin University 2012;18:315-319.
19. Merrill PRaE. Polymer Synthesis. Basel, Heidelberg, New York: Hüthig & Wepf, 1991.
20. Dubois P, Coulembier O, and Raquez J-M. Handbook of Ring-Opening Polymerization: John Wiley & Sons, 2009.
21. Chisholm M, Galucci J, Krempner C, and Wiggenhorn C. Dalton Transactions 2006(6):846-851.